BL09XU
HAXPES I

1. Introduction

BL09XU is an X-ray beamline with a 32-mm-period standard linear undulator. Until FY2020, the beamline had been a shared operation between nuclear resonant scattering and hard X-ray photoelectron spectroscopy (HAXPES). In FY2021, BL09XU took on the HAXPES activities previously carried out at BL47XU and was reorganized as a beamline dedicated to HAXPES [1]. In this upgrade, all optics, except for a liquid-nitrogen-cooled double-crystal monochromator with Si 111 reflection, were upgraded to state-of-the-art ones specialized for HAXPES experiments for conducting more advanced HAXPES applications, such as resonant HAXPES [2] and three-dimensional spatially resolved chemical bonding analysis [3]. For example, two pairs of double-channel cut crystal monochromators with Si 220 and Si 311 reflections were introduced to realize HAXPES analyses with total energy resolution below 300 meV at any incident photon energy of 4.9–12 keV while satisfying a fixed-exit condition. X-ray phase retarders with two diamond crystals enable us to control the polarization state with a high polarization degree of above 0.9 in a wide energy range of 5.9–9.5 keV. The name of the beamline was changed to "HAXPES I".

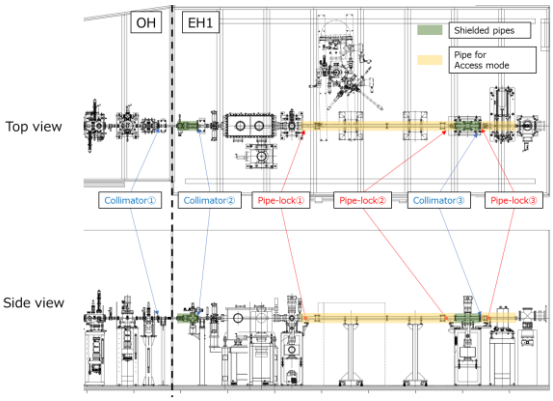

Fig. 1. Conceptual figure of "Access mode". When experiments are conducted in EH2, the HAXPES equipment in EH1 is retracted from the beam axis, and each device on the beam axis is connected by pipes for the "Access mode".

In FY2022, we introduced (1) a new operation mode, "Access mode", (2) a portable sample preparation chamber, and (3) a silicon drift detector (SDD) for fast sample positioning.

When experimental hutches (EHs) are arranged in tandem, it is difficult to perform maintenance of the system and sample preparation in the upstream hutch while experiments are being carried out downstream. Therefore, the new operation mode was introduced to allow access to EH1 even when an experiment is being conducted in the downstream EH2.

Pretreatments of samples expand the target application of the HAXPES analysis. For insulator samples, coating the sample surface with a metallic film is effective in suppressing charge-up. On the other hand, to analyze the electronic state in a region deeper than the detection depth of the HAXPES measurement, sputtering is used to scrape the surface. We have developed a system for various sample surface pretreatments, such as deposition and sputtering.

Two-dimensional mapping measurements of photoelectron intensity can be performed by combining the use of a focused beam with sample

scanning in both HAXPES instruments. The photoelectron intensity is directly obtained using the "PEAK" software from SCIENTA OMICRON, and sample scanning is performed using the BL-774 system [4]. On the other hand, since X-ray fluorescence can be detected more efficiently than photoelectrons, the time required for mapping measurements can be reduced by using fluorescence detection. Therefore, SDD was introduced to enable X-ray fluorescence detection in the EH2 system, which is designed to use a 1 μm beam focused by Kirkpatrick–Baez (KB) focusing mirrors.

2. New Operation Mode: "Access mode"

A new operation mode that allows full-time access to EH1 even when experiments are being conducted in the downstream EH2 has been developed. The HAXPES equipment in EH1 is mounted on rails and can be easily retracted from the beam axis. After retracting the equipment, vacuum pipes are installed along the beam axis to guide the beam to EH2 through a vacuum path without any strong X-ray scatterers, such as optical devices, valves, and high-density gasses. Note that the pipes are not radiation-shielded to facilitate the installation of the pipes. For safe access in EH1, (1) some collimators are placed in both OH and EH1 to prevent X-rays scattered from objects in OH from hitting nonshielded equipment in EH1, and (2) an interlock system was developed to ensure that no strong X-ray scatterers exist along the beam axis in EH1. These were carried out by Osaka (RIKEN) *et al.* referring to the system already in use at SACLA BL3.

A new local interlock system has been developed in addition to the beamline interlock system, and it monitors the condition of the equipment that may possibly be inserted into the beam axis. In addition, the local interlock system also checks that the beam path is set correctly. When the interlock conditions are broken, signals are sent to the beamline interlock to shut off the beam immediately. The introduction of this operation mode not only allows safe and full-time access to EH1 and enables the EH1 equipment to be kept in good condition, but also allows time-consuming preparations to be carried out in advance so that HAXPES measurements can be performed as soon as the EH1 experiment is ready.

3. Portable Sample Preparation Chamber

Both HAXPES instruments at BL09XU are equipped with a fracture tool and a file to obtain clean surfaces under ultrahigh-vacuum (UHV) environments. For more advanced sample preparation, a portable sample preparation chamber was developed. The preparation chamber can be operated in a UHV environment, for example, to remove surface contamination by sputtering or to reduce charge-up by depositing conductive films. Because it takes a long time to perform complex surface treatments, efficient HAXPES measurements are realized if the samples are treated off-line in advance and introduced into the EH1 and EH2 chambers without being exposed to the atmosphere.

A drawing of the portable preparation chamber is shown in Fig. 2. This chamber is equipped with a nonevaporable getter (NEG) pump in addition to a turbomolecular pump, enabling the chamber to maintain a UHV environment of about 10^{-8} Pa while moving the chamber. It is also equipped with an ion gun for Ar sputtering. A radio-frequency sputter gun is used as the deposition source, and a

Fig. 2. Portable sample preparation chamber for HAXPES equipment.

quartz crystal monitor is installed in front of the gun for controlling film thickness. Samples can be heated up to 500 °C by a ceramic heater on the back. Furthermore, by changing to an electron bombardment heating head, heat treatment at an even higher temperature is possible. The surface condition can be observed with low-energy electron diffraction (LEED)/Auger electron spectroscopy (AES) spectrometers to analyze the surface periodic structure and components. Samples are manipulated using a 4-axis manipulator, the z- and θ-axes of which are precisely controlled by stepping motors.

As an example of the use of the preparation chamber, we show, in Fig. 3, the effect of reducing the charge-up of an insulator sample by depositing a Ru metal film. A HAXPES measurement of an MgO substrate, which is a typical insulator, was performed using the EH2 system. The MgO substrate before deposition did not show accurate peaks because of the charge-up effect. Next, the measured samples were coated with 1 μm of Ru in the preparation chamber connected to the EH2 system, and then measured again. A sharp peak of Mg 1s is observed at around 1300 eV in the deposited sample in addition to Ru peaks. This indicates that the deposition of conductive films reduced the charge-up effect, allowing us to obtain original signals of insulator samples in HAXPES with a deep detection depth. By performing such pretreatment in the preparation chamber, HAXPES can be used in a wider range of applications.

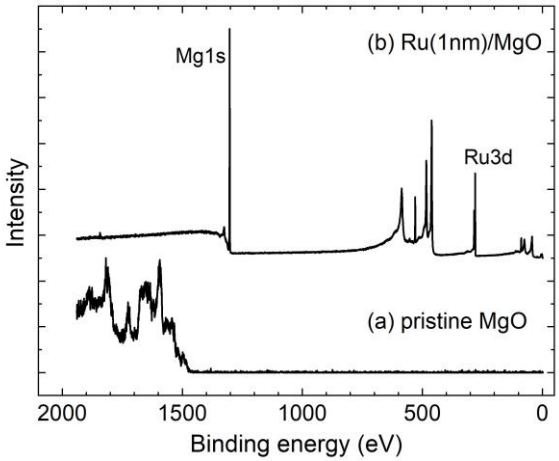

Fig. 3. Survey spectra of (a) pristine MgO substrate and (b) MgO substrate with 1 nm Ru film deposited.

4. SDD for Fast Sample Positioning

An SDD for UHV environments was introduced to the EH2 system. The EH2 analyzer is equipped with a photoelectron objective lens that enables photoelectron collection at a wide angle of ±32°. The distance between the objective lens and the sample is very narrow (13 mm), and the objective lens protrudes very close to the sample. Therefore, the existing ports in the measurement chamber had significant limitations on the conditions under which fluorescent X-rays from the sample could be detected. An SDD compatible with the UHV

environment enables efficient detection of fluorescent X-rays, since it can be installed at any place in the measurement chamber. The introduced SDD has UHV specifications and is equipped with a visible light cutoff film by AMPTEK [Fig. 4(a)].

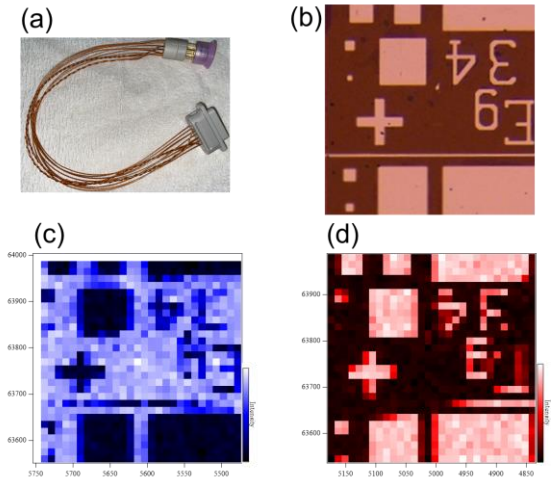

Fig. 4. (a) Photograph of the installed SDD. (b) Laser microscope image of an AlScN/TiN bilayer sample with TiN electrodes. (c) Photoelectron intensity map of Al 1s. (d) Fluorescence intensity map of Ti Kα.

An example of scanning two-dimensional mapping by simultaneous measurement of photoelectron and fluorescence using an SDD with the same performance as the introduced SDD is shown in Figs. 4(b)–4(d). The measured sample was provided by Prof. Nohira (Tokyo City Univ.) and consisted of an AlScN/TiN bilayer film with TiN electrodes [Fig. 4(b)]. Mapping data for the intensity of Al 1s photoelectrons and Ti Kα fluorescence in this sample are shown in Figs. 4(c) and 4(d), respectively. The fluorescence mapping shows high intensity in the area corresponding to the TiN electrode, while the photoelectron measurement shows the opposite pattern. An Sc Kα fluorescence mapping was also obtained at the same time, and its intensity is almost uniform (not shown). This is due to the small thickness of the TiN layer of the top electrode, and indicates the bulk sensitivity of fluorescence detection. Thus, the advantage of fluorescence detection is that not only can the intensity be obtained with high efficiency, the distribution of each constituent element can also be obtained simultaneously. Furthermore, as mentioned above, photoelectron and fluorescence have different detection depths. It is also expected that more accurate positioning will be possible when combined with photoelectron detection.

Yasui Akira and Takagi Yasumasa
Advanced Spectroscopy Team, Spectroscopy Division, JASRI

References:

[1] Yasui, A. & Takagi, Y. (2022). *SPring-8/SACLA Annual Report FY2021*, 31.

[2] For example, Maeda, K. Sato, H. Akedo, Y. Kawabata, T. Abe, K. Shimokasa, R. Yasui, A. Mizumaki, M. Kawamura, N. Ikenaga, E. Tsutsui, S. Matsumoto, K. Hiraoka, K. & Mimura, K. (2020). *JPS Conf. Proc.* **30**, 011137.

[3] For example, Oshime, N. Kano, J. Ikenaga, E. Yasui, S. Hamasaki, Y. Yasuhara, S. Hinokuma, S. Ikeda, N. Janolin, P. E. Kiat, J. M. Itoh, M. Yokoya, T. Fujii, T. Yasui, A. & Osawa, H. (2020). *Sci. Rep.* **10**, 10702.

[4] Nakajima, K. Motomura, K. Hiraki, T. N. Nakada, K. Sugimoto, T. Watanabe, K. Osaka, T. Yamazaki, H. Ohashi, H. Joti, Y. Hatsui T. & Yabashi, M. (2022). *J. Phys.: Conf. Ser.* **2380**, 012101.